RSC Advances

PAPER

View Article Online
View Journal | View Issue

Cite this: *RSC Adv.*, 2024, **14**, 10653

A microcapsule-based reusable self-reporting system using a donor–acceptor Stenhouse adduct†

Soonyoung Choi,‡[a] Gyeong Eun Kim,‡[a] Hyoungeun Bae,‡[a] Su Jeong Choi,[a] Ji-Eun Jeong,[a] Jin Chul Kim,[a] Hanah Na,[a] Hyocheol Jung,*[a] Yu Jin Jung,*[a] Sang-Ho Lee*[ab] and Young Il Park*[a]

Self-reporting systems automatically indicate damaged or corroded surfaces *via* color changes or fluorescence. In this study, a novel reusable self-reporting system is developed by exploiting the reversibility of a donor–acceptor Stenhouse adduct (DASA). The synthesized DASA precursor exhibits a color change when damaged upon reaction with diethylamine, and returns to its colorless form upon irradiation with visible light. Microcapsules are synthesized with a core comprising styrene and the DASA precursor, along with a shell formed of urea and formaldehyde. The optimal particle size and shell thickness of the microcapsules are 225 μm and 0.17 μm, respectively. The DASA precursor-containing microcapsules are embedded in a PEG gel matrix with secondary amine groups. This coating system, initially colorless, exhibits a color change, becoming pink after being damaged by scratching due to the reaction between the DASA precursor released from ruptured microcapsules with the secondary amine groups of the PEG gel, thus demonstrating self-reporting characteristics. Furthermore, the colored surface is restored to its initial colorless state by irradiation with visible light for 1.5 hours, demonstrating the reusability of the self-reporting system.

Received 5th February 2024
Accepted 14th March 2024

DOI: 10.1039/d4ra00925h

rsc.li/rsc-advances

1. Introduction

Coating technologies are a cornerstone in modern materials science, playing a vital role in safeguarding substrates against damage and corrosion. These coatings are more than just protective layers; they are integral to prolonging the lifespan of products across various industries, thereby contributing significantly to public safety and the longevity of infrastructure and consumer goods. Damage and corrosion are pervasive issues that can significantly reduce the lifecycle of both the coating itself and the underlying product. The advent of smart coating technologies marks a paradigm shift in this domain, introducing innovations like self-reporting, self-healing, and self-cleaning systems.[1–5] These advanced systems are key to extending the life cycle of products, ensuring they maintain their integrity and functionality over extended periods.

Self-reporting systems are especially noteworthy. Their primary function is to autonomously indicate the presence of damage or corrosion on a surface. This is often achieved through a visual change, such as a shift in color or the emission of fluorescence, alerting maintenance personnel to the need for timely repairs. This feature is crucial in preventing minor damage from escalating into major, potentially catastrophic failures. To implement autonomous reporting of damages, a variety of self-reporting technologies have been explored and developed. These include embedding microcapsules,[6,7] mechanophores,[8,9] specialized fibers,[10,11] and sensor molecules[12,13] in polymer matrices. Each of these technologies offers unique benefits and challenges in the detection and visualization of damage.

Dye-filled microcapsules are a prominent example of such technologies. Their straightforward approach to damage detection allows for the easy visualization of harm without requiring complex, specialized equipment.[14] This simplicity makes them particularly appealing for widespread application. Various types of dyes have been utilized in these microcapsules, including polyacetylene,[15] xanthene,[14] tetraphenylethylene (TPE),[16] and phenanthroline derivatives.[17] These dyes act as indicators, changing color to signal damage. However, a significant limitation of these systems is their one-time use nature. Once they signal damage by changing color, they cannot revert to their original state, which restricts their long-term applicability and increases maintenance costs.

In response to this limitation, researchers have been investigating coating systems that not only display a color change to report damage but can also return to their original color,

[a]*Center for Advanced Specialty Chemicals, Korea Research Institute of Chemical Technology, Ulsan, 44412, Republic of Korea. E-mail: hjung@krict.re.kr; yjjung@krict.re.kr; slee@krict.re.kr; ypark@krict.re.kr*

[b]*Department of Chemical & Biochemical Engineering, Dongguk University, Seoul, 04620, Republic of Korea*

† Electronic supplementary information (ESI) available. See DOI: https://doi.org/10.1039/d4ra00925h

‡ These authors contributed equally to this work.

enhancing the reusability and functionality of self-reporting technologies. For instance, Hu *et al.* reported the development of a color-detectable self-reporting nanocapsule-based system that uses crystal violet lactone as an indicator. While innovative, this system requires the introduction of additional decoloring chemical agents, such as ethanol, diethylenetriamine, and multivalent alkynes,[18] to revert to its original state. Similarly, Jung *et al.* introduced a reusable damage-detection and self-healing system based on the Diels–Alder reaction using spiropyran. This system, though a step forward, necessitates the application of high temperatures (approximately 120 °C) directly to the damaged surface to restore it to its initial state.[19]

These developments, while indicative of significant progress, underscore the ongoing challenges in the field of smart coatings. The ideal self-reporting system remains elusive one that is not only effective in signaling damage but also capable of multiple cycles of reporting and self-repair, all while being environmentally sustainable and cost-effective. The pursuit of such a system continues to drive research, opening up new frontiers in materials science. The potential applications of such advanced coatings are vast, ranging from aerospace and automotive industries to consumer electronics and infrastructure. The development of more efficient, durable, and reusable smart coatings could have far-reaching implications, leading to safer, more sustainable, and longer-lasting products and structures.

This ongoing quest for innovation in smart coating technologies is fueled by the increasing demand for materials that can withstand harsher environments, more intense usage, and longer lifespans. Researchers and industry experts are

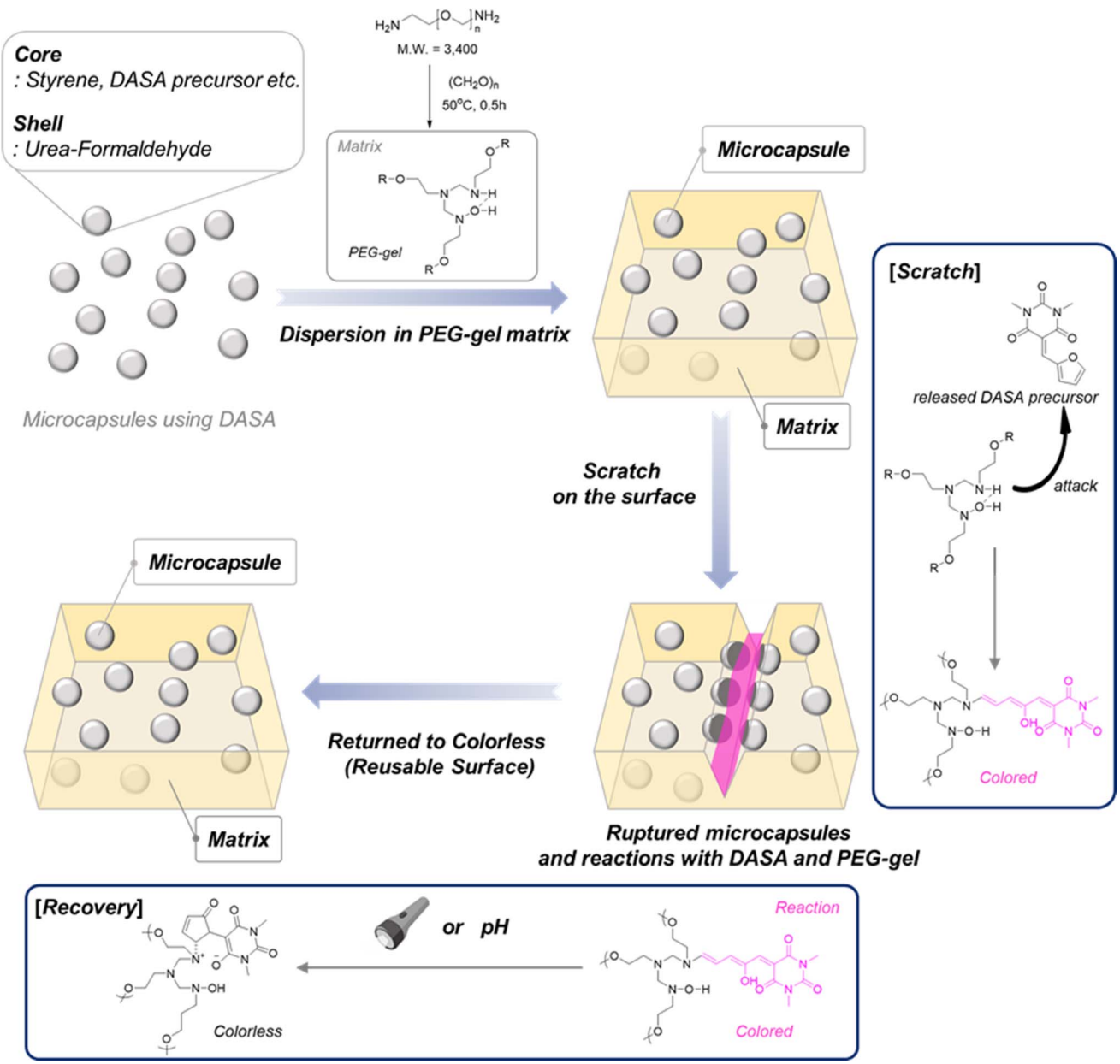

Fig. 1 Schematic illustration of the microcapsule-based reusable self-reporting system using the DASA dye.

continually exploring new materials, chemical formulations, and nanotechnology applications to achieve these goals. The future of smart coatings looks promising, with the potential to revolutionize how we protect, maintain, and extend the life of a myriad of products and structures in our daily lives. As this field continues to evolve, it holds the promise of not only addressing the current limitations but also opening up new possibilities for protecting and preserving the world around us in more intelligent and efficient ways.

In this comprehensive study, we have successfully developed and demonstrated a cutting-edge, microcapsule-based reusable self-reporting coating system. This system, as depicted in Fig. 1, innovatively employs a donor–acceptor Stenhouse adduct (DASA) as its dye component. The unique attribute of this DASA dye is its ability to undergo reversible color changes when subjected to external stimuli, such as thermal energy or light irradiation.[20] This feature is pivotal, as it ensures the reusability of the self-reporting coating, a significant advancement over previous technologies.

The design of these microcapsules is intricate. At their core, they contain styrene along with the DASA precursor, which acts as the indicating agent.[21–24] This combination is crucial for the function of the microcapsules, as the DASA precursor is the component that undergoes a color change in response to damage. The shell of the microcapsules is composed of a blend of urea and formaldehyde. This composition is carefully selected to provide optimal protection and stability to the core components. Additionally, the shell thickness plays a critical role in the overall performance of the microcapsules. It is meticulously optimized by varying the amount of poly(ethylene-*alt*-maleic anhydride) (PEMA), which is used to enhance the microcapsules' stability under various extrinsic forces. Incorporated into this system is a polyethylene glycol (PEG) gel, selected for its reactive properties with the DASA precursor. This gel is infused with secondary amine groups, which are essential for the interaction with the DASA precursor. When the coating surface is compromised, such as by a scratch, the DASA precursor is released from the microcapsules. Upon release, it reacts with the PEG gel, triggering a color change from colorless to pink. This color change serves as a clear and immediate indication of damage, fulfilling the self-reporting function of the coating.

Remarkably, the innovation of this system doesn't stop with damage detection. The true novelty lies in its ability to revert to its original state. Upon exposure to light irradiation for a duration of 1.5 hours, the colored surface transitions back to its original, colorless state. This reversible behavior is a significant improvement over traditional systems, which either require additional decoloring agents or do not revert at all. In this comprehensive study, we have successfully developed and demonstrated a cutting-edge, microcapsule-based reusable self-reporting coating system. This system, as depicted in Fig. 1, innovatively employs a DASA as its dye component. The unique attribute of this DASA dye is its ability to undergo reversible color changes when subjected to external stimuli, such as thermal energy or light irradiation. This feature is pivotal, as it ensures the reusability of the self-reporting coating, a significant advancement over previous technologies.

2. Experimental

2.1. Materials

Urea was acquired from Alfa Aesar. An aqueous formaldehyde solution (37 wt%), poly(ethylene-*alt*-maleic anhydride) (EMA), resorcinol, ammonium chloride, NaOH, and 1-octanol were purchased from Sigma-Aldrich. Styrene, purchased from the Samchun Pure Chemical Co, was passed through a basic alumina column to remove inhibitors. All other reagents and solvents were used as received without further purification, including paraformaldehyde (Sigma-Aldrich; 95%), polyoxyethylene bis(amine) (Thermo Scientific; MW 3400), and *n*-methyl-2-pyrrolidone (NMP; Daejung Chemicals & Metals; ≥99.5%).

2.2. Instruments

^{1}H-NMR spectra were recorded using a Bruker Ultrashield 300 MHz spectrometer. Ultraviolet-visible-near infrared (UV-vis-NIR) absorption spectra were measured using a JASCO V-700 spectrometer (1 cm cuvette cell). A mechanical stirrer (EUROSTAR 20, IKA) was used for microencapsulation. Images of the microcapsules and the damaged and healed surface were obtained using an optical microscope (BX-53, Olympus). Microcapsule size was analyzed using a microscope equipped with a CCD camera (DP73, Olympus) and image analysis software (CellSens Entry, Olympus). The mean diameter was determined from a dataset containing at least 300 individual diameter measurements. Scanning electron microscopy (SEM, SNE-3000M, SEC) was used to examine the morphology, shape, and surface coating of the microcapsules. Photographs were taken using a microscope and a digital camera (NX 3000, Samsung). The particle size distributions of microcapsules were determined using a laser particle size analyzer (Malvern Mastersizer 3000), with a range of 0.1–1000 μm. Thermal analysis of the microcapsules was performed using Q500 TA Instruments upon heating from 25 °C to 600 °C, with a heating rate of 10 °C min^{-1} in a nitrogen atmosphere.

2.3. Synthesis and characterization of the DASA dye

2.3.1. 5-(Furan-2-ylmethylene)-1,3-dimethylpyrimidine-2,4,6(1*H*,3*H*,5*H*)-trione (1). 1,3-Dimethylbarbituric acid (10.0 mmol) and furfural (10.0 mmol) were dissolved in H_2O (20.0 mL) and the solution was stirred for 2 hours. The precipitated yellow solid was filtered and washed several times with cold water. After extraction with dichloromethane (DCM)/aqueous $NaHSO_3$, the organic layer was completely dried using $MgSO_4$. All solvents were evaporated by vacuum distillation under reduced pressure to obtain compound (**1**). Yield 83.0% ^{1}H NMR ($CDCl_3$, 300 MHz) δ 8.65 (d, 1H), 8.45 (s, 1H), 7.87 (d, 1H), 6.76 (tri, 1H), 3.41 (s, 6H).

2.3.2. 5-((2*Z*,4*E*)-5-(Diethylamino)-2-hydroxypenta-2,4-dien-1-ylidene)-1,3-dimethylpyrimidine-2,4,6(1*H*,3*H*,5*H*)-trione (2): donor–acceptor Stenhouse adducts (DASA). Compound (**1**)

(10.0 mmol) and diethyl amine (10.0 mmol) were dissolved in DCM (20.0 mL). Then, the mixture was stirred at room temperature for 30 minutes, cooled to 0 °C and stirred for a further 30 minutes. The mixture was distilled under reduced pressure to remove the solvent and precipitated with cold ether to obtain compound (2). Yield 71% ^{1}H NMR ($CDCl_3$, 300 MHz) δ 12.58 (s, 1H), 7.25 (s, 1H), 7.19 (d, 1H), 6.75 (d, 1H), 6.10 (tri, 1H), 3.52 (m, 4H), 3.38 (s, 6H), 1.36 (m, 6H).

2.4. Synthesis of microcapsules with the DASA dye

An aqueous solution of PEMA (25 wt%, 40.0 mL) was added to distilled water (85.0 mL), to which urea (2.51 g), resorcinol (0.250 g), and ammonium chloride (0.250 g) were added under stirring. The pH of the resultant solution was adjusted to 3.50 using an aqueous NaOH solution (10%). One drop of 1-octanol was added to eliminate the surface bubbles. The resulting mixture was agitated at 500 rpm, and the core material (44.7 g), which consisted of the DASA dye (0.200 g) and styrene (44.50 g = 49.0 mL) in a weight ratio of 1 : 221, was added to the stirred solution. A solution (37.0 wt%) of formaldehyde (7.19 g, 0.0892 mol) was added to the agitated emulsion. The resulting mixture was heated to 55 °C, and retained at that temperature for 5.5 hours. The reaction mixture was then cooled to room temperature, and the microcapsules were separated by vacuum filtration, washed with acetone and dichloromethane, and air-dried.

2.5. Encapsulation yield and encapsulation efficiency calculation

The encapsulation yield was calculated as the ratio of the obtained mass of microcapsules at the end of the reaction and the mass of initial substances added during the reaction. The encapsulation efficiency was calculated as the ratio between the mass of core materials to be encapsulated and its mass in the final product.

Overall encapsulation yield

$$\text{Yield}(\%) = \frac{W_e}{W_t} \times 100 = 61.84$$

W_e = obtained microcapsule mass = 31.65 g. W_t = total weight of substances added for microcapsule formation = W_{urea} + $W_{formaldehyde}$ + $W_{resorcinol}$ + $W_{styrene}$ + W_{EMA} + W_{DASA} = 2.51 g + 2.68 g + 0.25 g + 44.54 g + 1.00 g + 0.20 g = 51.18 g.

$$\text{Actual core content } C_a(\%) = \left(\frac{\Delta H_{fus}}{\Delta H_{styrene}}\right) \times 100 = 66.98(\text{styrene})$$

According to the weight ratio of styrene : DASA = 220.61 : 1, DASA = 0.30%

$$\Delta H_{fus(capsule\text{-}styrene)} = 25.82 \text{ J g}^{-1}$$

$$\Delta H_{fus(styrene)} = 10.96 \text{ kJ mol}^{-1} = 38.55 \text{ J g}^{-1}$$

$$\text{Theoretical core content } C_t(\%) = \left(\frac{W_{styrene+DASA}}{W_{styrene+DASA} + W_m}\right) \times 100 = 89.16$$

$W_{styrene+DASA}$ = 44.74 g. W_m = weight of monomer except core materials = W_{urea} + $W_{formaldehyde}$ + $W_{resorcinol}$ = 2.51 g + 2.68 g + 0.25 g = 5.44 g.

$$\text{Encapsulation efficiency } E(\%) = \left(\frac{C_a}{C_t}\right) \times 100 = 75.12$$

2.6. Preparation of PEG gel containing microcapsules

Polyoxyethylene bis(amine) (43.6 mmol; 0.222 g) and paraformaldehyde (220 mmol; 10.4 mg) were dissolved in NMP (1.42 mL). This solution was poured into a mold and half of it was cured for 30 minutes at 50 °C. Next, microcapsules constituting 20.0 wt% of the solution, weighing 0.356 g, were added to the remaining solution. This was then poured into the mold. To prevent the microcapsules from settling, we first poured and cured half of the solution. The microcapsules dispersed well and settled at the bottom of the mold after a few minutes. This mixture was cured for another 30 minutes at 50 °C, resulting in a yellow gel.

2.7. Demonstration of reusable self-reporting system

The obtained self-reporting gel was scratched vertically with a razor blade, producing a color change from colorless to pink. After 15 min, the scratched gel was irradiated with white light for 1.5 hours, whereupon the gel returned to its original color. The gel was then scratched horizontally and a color change was clearly observed.

3. Results and discussion

3.1. Synthesis and reversibility test of the DASA

The DASA precursor used to prepare the indicator in the self-reporting system was synthesized according to an established procedure (Fig. 2(a)).[20] The synthesis of the DASA precursor was confirmed by ^{1}H-NMR (Fig. S1(a)†). Furthermore, to verify the reversibility of the synthesized DASA precursor, a model DASA compound was synthesized with diethyl amine as the secondary amine moiety (Fig. 2(b)). The reaction between the DASA precursor and diethyl amine afforded linear DASA, as confirmed by ^{1}H-NMR (Fig. S1(b)†).

To confirm the reversible nature of linear DASA, comprehensive analyses were performed using UV-visible (UV-vis) absorption spectroscopy after subjecting the substance to heat treatment and visible light irradiation while in a solution state. Detailed in Fig. 3, this process illuminated the changes in the UV-vis absorption spectrum of linear DASA both before and after exposure to visible light. Initially, the UV-vis absorption spectrum for the colored linear DASA, as depicted by the red line in Fig. 3, prominently displayed a strong absorption peak at 570 nm. This peak is indicative of the DASA's colored state. However, following the irradiation of this colored linear DASA with visible light, a significant transformation in the absorption spectrum was observed. The spectrum, now represented by the

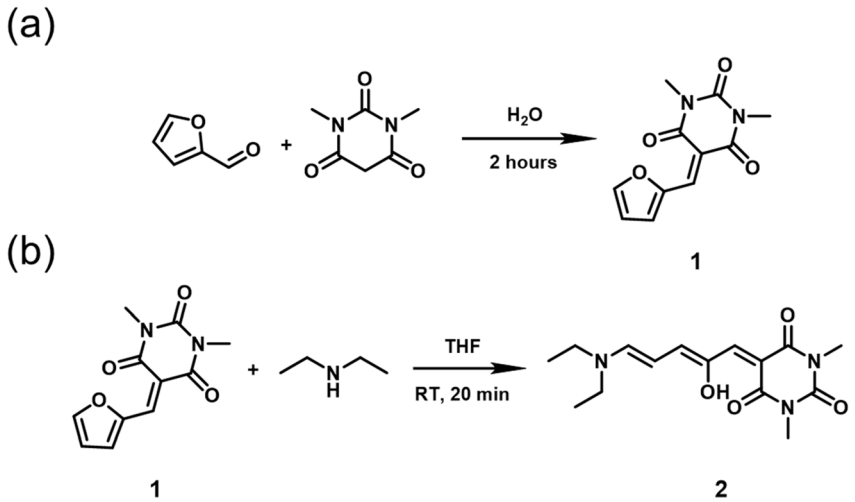

Fig. 2 (a) Synthesis of the DASA precursor; (b) synthesis of the linear DASA.

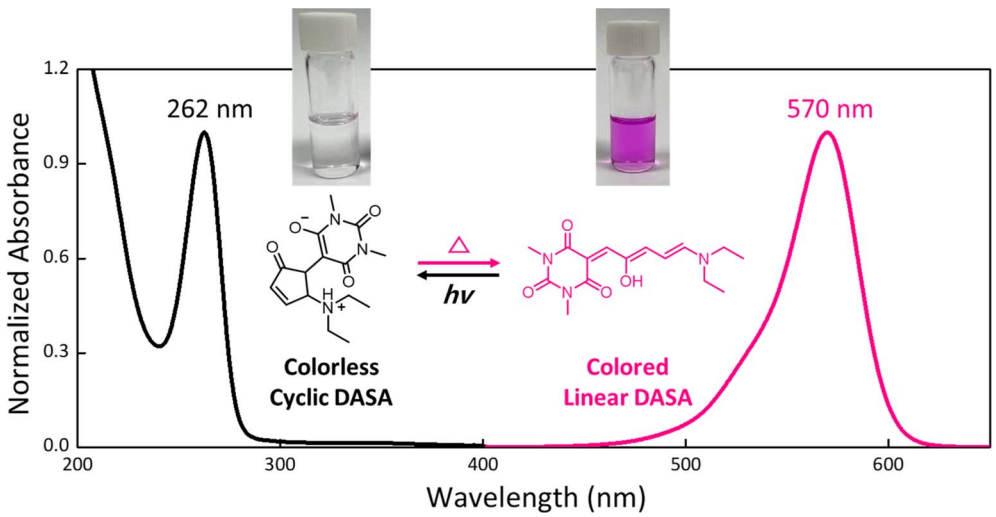

Fig. 3 Normalized UV-visible absorption spectra of the cyclic DASA in water (black line) and the linear DASA in toluene (red line).

black line, aligned closely with that of the colorless cyclic DASA. This alignment was marked by a pronounced absorption peak at 262 nm and the complete disappearance of the previous peak at 570 nm.

Furthermore, the application of heat to the cyclic DASA instigated a return to the original characteristics, both in terms of the UV-vis absorption spectrum and the color. This change back to the initial states post-heat application was a critical observation, further reinforcing the substance's reversible attributes. To provide additional verification of the structural changes between the linear and cyclic forms of DASA, ^{1}H-NMR spectroscopy was employed. The results, as shown in Fig. S1(a) and (b),† conclusively confirmed the reversible transformation between these two forms of DASA. Such findings are pivotal, as they clearly demonstrate the suitability of DASA as an effective indicator in a non-contact, reusable self-reporting system. This system could have significant implications for various applications where reversible, visual indication of state changes is vital.

3.2. Preparation and characterization of microcapsules with the DASA dye

Polyurea-formaldehyde (PUF) microcapsules encapsulating the DASA precursor and styrene, collectively termed as the "core materials", were meticulously crafted using *in situ* polymerization within an oil-in-water emulsion. This intricate process entailed blending an aqueous solution composed of urea, resorcinol, formaldehyde, PEMA, and the core materials. The incorporation of resorcinol into the PUF shell was a deliberate move aimed at bolstering the shell's durability and enhancing the degree of cross-linking, a strategy underscored in multiple studies.[25–28] Additionally, PEMA played a dual role in this synthesis, functioning not only as a component of the shell but also as an emulsifier, as indicated in the literature.[29,30] Styrene, chosen for its low viscosity and low molecular weight, emerged as an ideal oil-phase material. Its potential as a repair agent is particularly noteworthy, given its minimal shrinkage and strong

adhesive properties when applied to various polymer composites.[31] This choice aligns with the trends observed in existing self-healing polymer composites, where styrene, because of its favorable properties, has been frequently utilized as a healing agent in systems based on microencapsulation technology.[31–34]

The surface morphology and shell thickness of the synthesized microcapsules were meticulously examined using Scanning Electron Microscopy (SEM). These microcapsules, produced under carefully optimized conditions involving EMA (40 mL) and styrene (49 mL), stirred at 500 rpm for a duration of 5.5 hours, presented a distinct morphology. They displayed a spherical shape, a smooth surface texture, and a uniform particle size distribution. The mean particle diameter, as observed in Fig. 4(a) and S2,† was determined to be approximately 225 μm. A critical aspect of these microcapsules was their shell thickness, which was measured to be 0.170 μm, as shown in Fig. S3, No. 1.† This thickness is a vital parameter, as it influences the stability and release rate of the core materials within the microcapsules, thereby directly impacting the efficiency and effectiveness of the self-healing and self-reporting functions of the encapsulated DASA and styrene. The uniformity in particle size and shell thickness are indicative of the precision and control achieved in the synthesis process, highlighting the potential for these microcapsules to be effectively utilized in a range of applications, especially in smart coatings where controlled release and precise responses to environmental changes are crucial.

The microencapsulation of the DASA dye was confirmed by NMR spectroscopy (Fig. S4†). The NMR spectrum of the ruptured microcapsules revealed chemical shifts corresponding to the DASA dye, confirming the successful encapsulation of the DASA dye within the PUF microcapsules.

The stable formation of microcapsules relies significantly on the ratio of shell-to-core materials, which is also known to be a critical factor in determining both the surface morphology and particle size of microcapsules. Excess shell material can result in particle aggregation, whereas insufficient shell material can cause the microcapsule to rupture during preparation.[35–37] To investigate the correlation between the core-to-shell ratio and microcapsule properties, the amount of styrene in the microcapsule core was systematically varied while holding all other preparation conditions constant (Table S1†). The SEM images and particle size distributions of the microcapsules with different styrene contents (ranging from 49 to 20 mL) are shown in Fig. S3 and S5,† respectively. The microcapsules exhibited uniform spherical shapes and smooth surfaces regardless of the styrene content. Neither particle aggregation nor microparticle collapse were observed, confirming the successful and stable formation of the microcapsules. Reducing the styrene content of the core materials resulted in microcapsules with a similar average size ranging from 197 μm to 256 μm. The capsule thickness also showed minimal variation with changes in the styrene content, ranging from 0.143 μm to 0.170 μm. Furthermore, the effect of the reaction time on the microcapsule size and thickness was negligible (Fig. S3 and S5†).

Considering the size, shell thickness, and yield, the optimal conditions for microcapsule synthesis involved 49.0 mL of styrene, 40.0 mL of PEMA, an agitation speed of 500 rpm, and a reaction time of 5.5 h (Table S2, entry 1†). The measured encapsulation efficiency of the microcapsules synthesized under this reaction condition, defined as the ratio of the actual core content to the theoretical core content, was 75.12%. Microcapsules produced under these optimized conditions were subsequently used for self-reporting applications. As shown in Fig. 4(b), the microcapsules synthesized with the optimal condition showed their stability to diethylamine, only exhibiting the color change after rupture by force.[38]

The thermal stability of the synthesized microcapsules was investigated through thermogravimetric analysis (TGA) (Fig. S6†). At temperatures below 150 °C, a slight weight loss is attributed to the evaporation of residual moisture and formaldehyde.[39,40] Significant weight loss around 235 °C is associated

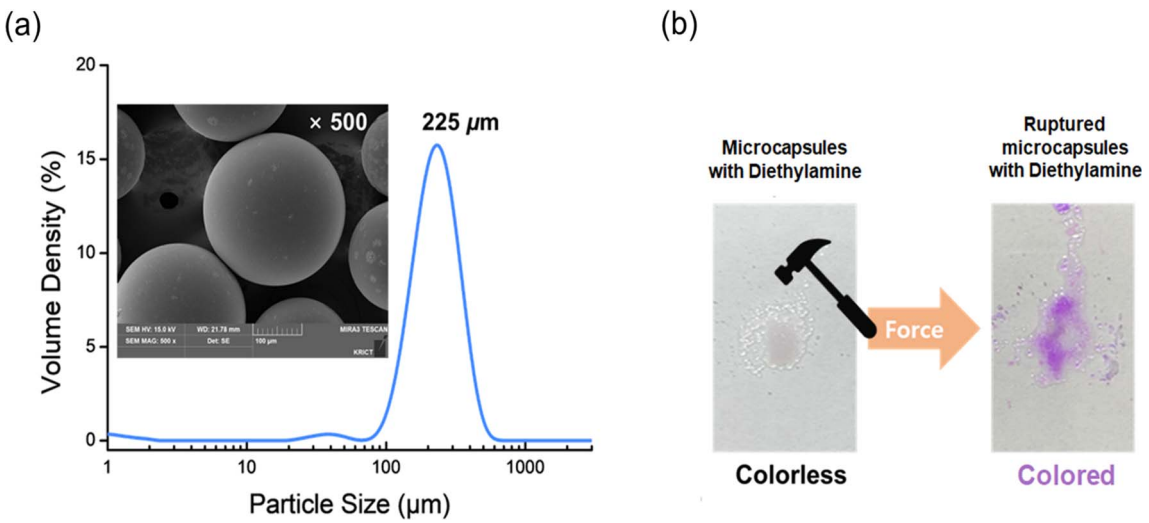

Fig. 4 (a) Particle size distribution of the synthesized microcapsules (inset: SEM image of the synthesized micro-capsules) and (b) photographs of the microcapsules before and after rupture and subsequent reaction with diethylamine.

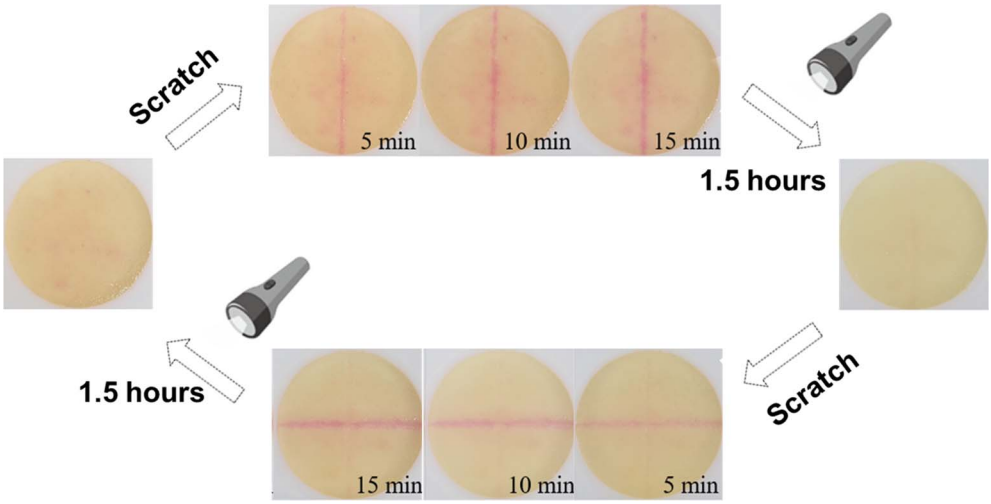

Fig. 5 Photographs demonstrating the microcapsule-based reusable self-reporting system using the DASA dye.

with the decomposition of the PUF microcapsule shell and organic core materials.[40,41] At higher temperatures above 350 °C, a substantial weight loss is observed, primarily due to the decomposition of homopolymerized encapsulated styrene core materials.[42] The temperature at which 6 wt% weight loss occurs is approximately 235 °C, demonstrating the thermal stability of the prepared microcapsules.

3.3. Demonstration of the microcapsule-based reusable self-reporting system

The microcapsules were strategically integrated into a PEG gel matrix to showcase the reusability of the self-reporting system. This integration was a pivotal step in demonstrating the system's practical applications. The first test to evaluate this involved deliberately damaging the surface of the self-reporting coating. This was done by creating a vertical scratch from top to bottom using a razor blade. Following this, the evolution of the color on the damaged area was closely monitored over time. The manifestation of color on the surface, as captured in Fig. 5, was a direct result of the DASA precursor being released from the ruptured microcapsules. Once released, the DASA precursor interacted with the secondary amines present in the PEG gel, leading to the observed color change. Notably, the color of the scratch intensified gradually, indicating the ongoing reaction between the released DASA precursor and the PEG gel.

To revert the damaged surface back to its original state and thus restore the coating surface to a functional condition, the coated area was subjected to visible light irradiation for a duration of 1.5 hours. This exposure to light triggered a chemical transformation, converting the colored linear DASA back to its colorless cyclic form. As a result, the coating surface regained its initial, fully decolorized state, thereby illustrating the system's self-repair capability.

In a second experimental setup, a horizontal scratch test was performed, extending from left to right across the coating surface. This test was designed to further assess the system's consistency and repeatability in response to damage. Similar to the first test, the color change in the damaged area was clearly visible due to the colored linear DASA. This again was the consequence of the DASA precursor's reaction with the PEG gel following the rupture of the microcapsules. Consistent with the results of the first test, irradiation of the damaged area with visible light for the same duration of 1.5 hours successfully restored the surface to its original condition.

These experiments, taken together, demonstrate the robustness and reliability of the microcapsule-based self-reporting system using the DASA dye. The system not only exhibits a clear self-reporting function by visibly indicating the presence of damage but also showcases its reusability through the ability to recover its original state post-damage. This dual functionality of reusability and self-reporting is essential for a wide range of applications, particularly in contexts where long-term durability and minimal maintenance are critical. The successful implementation of this system highlights the potential of smart coatings in various industries, paving the way for more sustainable and efficient material maintenance solutions.

4. Conclusion

In conclusion, this study has successfully unveiled a pioneering microcapsule-based reusable self-reporting system, employing the DASA dye as a discernible color agent embedded within a resilient PEG gel matrix. The meticulously designed microcapsules, featuring a core blend of styrene and the DASA precursor encased in a urea and formaldehyde shell, demonstrated robust stability, as corroborated by the precisely optimized thickness using varying PEMA quantities. Our investigation, supported by comprehensive laser diffraction data indicating an average microcapsule size of 255 μm, showcased the efficacy of the proposed self-reporting system. The integration of DASA precursor-laden microcapsules into a PEG gel matrix enriched with secondary amine groups exemplified remarkable reusability. The initial colorless state of the coating

transformed into a vibrant pink hue upon damage, underscoring the self-reporting characteristics facilitated by the chemical interaction between the liberated DASA precursor and the secondary amine groups of the PEG gel. Furthermore, the successful restoration of the colored surface to its original colorless state through a carefully orchestrated 1.5 hours exposure to visible light highlighted the system's exceptional durability and reusability. This innovative microcapsule-based self-reporting system not only offers convenience and easy retrieval but also plays a pivotal role in extending product life cycles and upholding public safety across various applications. These findings contribute significantly to the field, presenting a sophisticated and efficient self-reporting mechanism with implications for diverse industries. The integration of DASA dye and PEG gel matrix showcases a versatile approach with broad potential, emphasizing the system's adaptability and robustness for real-world applications. The novel insights and technological advancements presented in this study pave the way for further research and development in the realm of self-reporting systems, promising sustained contributions.

Conflicts of interest

There are no conflicts to declare.

Acknowledgements

This work was supported by the KRICT (KS2441-10), an institution of the National Research Foundation of Korea (NRF). This research was funded by the Technology Innovation Program of the Ministry of Trade, Industry and Energy (MOTIE, Korea; grant number 20011133). This work was supported by Korea Environment Industry & Technology Institute (KEITI) through project to develop eco-friendly new materials and processing technology derived from wildlife project, funded by Korea Ministry of Environment (MOE) (202100327004).

References

1 D. H. Son, H. E. Bae, M. J. Bae, S.-H. Lee, I. W. Cheong, Y. I. Park, J.-E. Jeong and J. C. Kim, *ACS Appl. Polym. Mater.*, 2022, **4**, 3802–3810.
2 J.-E. Jeong, J.-W. Lee, M. J. Bae, H. E. Bae, E. Seo, S. Lee, J. Y. Shin, S.-H. Lee, Y. J. Jung, H. Jung, Y. I. Park, I. W. Cheong, H.-R. Kim and J. C. Kim, *ACS Appl. Mater. Interfaces*, 2023, **15**, 8510–8520.
3 M. E. Grady, B. A. Beiermann, J. S. Moore and N. R. Sottos, *ACS Appl. Mater. Interfaces*, 2014, **6**, 5350–5355.
4 S. Chae, J. P. Lee and J.-M. Kim, *Adv. Funct. Mater.*, 2016, **26**, 1769–1776.
5 M. Li, Q. Zhang and S. Zhu, *Polymers*, 2016, **99**, 521–528.
6 M. J. Robb, W. Li, R. C. R. Gergely, C. C. Matthews, S. R. White, N. R. Sottos and J. S. Moore, *ACS Cent. Sci.*, 2016, **2**, 598–603.
7 Y. K. Song, T. H. Lee, K. C. Lee, M. H. Choi, J. C. Kim, S.-H. Lee, S. M. Noh and Y. I. Park, *Appl. Surf. Sci.*, 2020, **511**, 145556.
8 M. Li, Q. Zhang, Y.-N. Zhou and S. Zhu, *Prog. Polym. Sci.*, 2018, **79**, 26–39.
9 R. W. Barber, M. E. McFadden, X. Hu and M. J. Robb, *Synlett*, 2019, **30**, 1725–1732.
10 S. Shree, M. Dowds, A. Kuntze, Y. K. Mishra, A. Staubitz and R. Adelung, *Mater. Horiz.*, 2020, **7**, 598–604.
11 A. D. Das, G. Mannoni, A. E. Früh, D. Orsi, R. Pinalli and E. Dalcanale, *ACS Appl. Polym. Mater.*, 2019, **1**, 2990–2997.
12 X. Zheng, Q. Wang, Y. Li, J. Luan and N. Wang, *Adv. Mater. Technol.*, 2020, **5**, 1900832.
13 M. Amjadi and M. Sitti, *Adv. Sci.*, 2018, **5**, 1800239.
14 W. Li, C. C. Matthews, K. Yang, M. T. Odarczenko, S. R. White and N. R. Sottos, *Adv. Mater.*, 2016, **28**, 2189–2194.
15 S. A. Odom, A. C. Jackson, A. M. Prokup, S. Chayanupatkul, N. R. Sottos, S. R. White and J. S. Moore, *ACS Appl. Mater. Interfaces*, 2011, **3**, 4547–4551.
16 Y. K. Song, B. Kim, T. H. Lee, J. C. Kim, J. H. Nam, S. M. Noh and Y. I. Park, *Macromol. Rapid Commun.*, 2017, **38**, 1600657.
17 G. S. Dhole, G. Gunasekaran, S. K. Singh and M. Vinjamur, *Prog. Org. Coat.*, 2015, **89**, 8–16.
18 M. Hu, S. Peil, Y. Xing, D. Döhler, L. C. Caire da Silva, W. H. Binder, M. Kappl and M. B. Bannwarth, *Mater. Horiz.*, 2018, **5**, 51–58.
19 S. Jung, H. G. Jang, J. Y. Jo, Y. S. Kim, D. C. Lee and J. Kim, *ACS Appl. Mater. Interfaces*, 2023, **15**, 26028–26036.
20 S. Helmy, F. A. Leibfarth, S. Oh, J. E. Poelma, C. J. Hawker and J. R. Alaniz, *J. Am. Chem. Soc.*, 2014, **136**, 8169–8172.
21 V. Naveen, A. P. Deshpande and S. Raja, *RSC Adv.*, 2020, **10**, 33178–33188.
22 N. Veeramani, R. Samikannu, A. P. Deshpande, S. Varghese and V. Moses, *Int. Polym. Process.*, 2023, **1**, 1–13.
23 C. Zhao, Y. Zhu, B. Kong, Y. Huang, D. Yan, H. Tan and L. Shang, *ACS Appl. Mater. Interfaces*, 2020, **12**, 42586–42594.
24 V. Naveen, S. Raja and A. P. Deshpande, *Int. J. Plast. Technol.*, 2019, **23**, 157–169.
25 R. K. Hedaoo, P. P. Mahulikar and V. V. Gite, *Polym. Plast. Technol. Eng.*, 2013, **52**, 243–249.
26 K. Zhang, Q. Zhou and H.-M. Ye, *Appl. Sci.*, 2019, **9**, 599.
27 E. Scopelitis and A. Pizzi, *J. Appl. Polym. Sci.*, 1993, **48**, 2135–2146.
28 E. Scopelitis and A. Pizzi, *J. Appl. Polym. Sci.*, 1993, **47**, 351–360.
29 C. Fan and X. Zhou, *Polym. Bull.*, 2011, **67**, 15–27.
30 J. Liu, Y. Wu, W. Zhang, J. Long, P. Zhou and X. Chen, *Polymers*, 2019, **11**, 199.
31 Z. Li, H. Chen, Q. Xu, X. Li, H. Ma and Q. Yuan, *J. Coat. Technol. Res.*, 2022, **19**, 1837–1850.
32 H. Wang, Y. Yuan, M. Rong and M. Zhang, *Colloid Polym. Sci.*, 2009, **287**, 1089–1097.
33 H. P. Wang, *Adv. Mater. Res.*, 2011, **393–395**, 1279–1282.
34 *Composite and Functionally Graded Materials*, ed. J. N. Katsube and W. Jones, 1997, vol. 80, pp. 265–275.
35 B. Liu, A. R. R. Mazo, P. A. Gurr and G. G. Qiao, *ACS Appl. Mater. Interfaces*, 2020, **12**, 9782–9789.
36 H. Fukuo and T. Onoguchi, Microcapsule manufacture, *US Pat.*, 4753759A, 1988.

37 M. Li, B. Cao, R. Shang, H. Mei and L. Wang, *J. Appl. Polym. Sci.*, 2022, **139**, e53021.
38 O. I. Vinogradova, O. V. Lebedeva and B.-S. Kim, *Annu. Rev. Mater. Res.*, 2006, **36**, 143–178.
39 X.-x. Zhang, X.-m. Tao, K.-l. Yick and X.-c. Wang, *Colloid Polym. Sci.*, 2004, **282**, 330–336.
40 L. Yuan, G. Liang, J. Q. Xie, L. Li and J. Guo, *Polymer*, 2006, **47**, 5338–5349.
41 G. Farzi, A. Davoodi, A. Ahmadi, R. E. Neisiany, M. K. Anwer and M. A. Aboudzadeh, *ACS Omega*, 2021, **6**, 31147–31153.
42 H. P. Wang, Y. C. Yuan, M. Z. Rong and M. Q. Zhang, *Adv. Mater. Res.*, 2008, **47–50**, 286–289.